

Aberystwyth University

Accelerating fishes increase propulsive efficiency by modulating vortex ring geometry

Akanyeti, Otari; Putney, Joy; Yanagitsuru, Yuzo R.; Lauder, George V.; Stewart, William J.; Liao, James C.

Published in:

Proceedings of the National Academy of Sciences of the United States of America

DOI:

[10.1073/pnas.1705968115](https://doi.org/10.1073/pnas.1705968115)

Publication date:

2017

Citation for published version (APA):

Akanyeti, O., Putney, J., Yanagitsuru, Y. R., Lauder, G. V., Stewart, W. J., & Liao, J. C. (2017). Accelerating fishes increase propulsive efficiency by modulating vortex ring geometry. *Proceedings of the National Academy of Sciences of the United States of America*, 114(52), 13828-13833. <https://doi.org/10.1073/pnas.1705968115>

General rights

Copyright and moral rights for the publications made accessible in the Aberystwyth Research Portal (the Institutional Repository) are retained by the authors and/or other copyright owners and it is a condition of accessing publications that users recognise and abide by the legal requirements associated with these rights.

- Users may download and print one copy of any publication from the Aberystwyth Research Portal for the purpose of private study or research.
- You may not further distribute the material or use it for any profit-making activity or commercial gain
- You may freely distribute the URL identifying the publication in the Aberystwyth Research Portal

Take down policy

If you believe that this document breaches copyright please contact us providing details, and we will remove access to the work immediately and investigate your claim.

tel: +44 1970 62 2400

email: is@aber.ac.uk

**ACCELERATING FISHES INCREASE PROPULSIVE EFFICIENCY BY
MODULATING VORTEX RING GEOMETRY.**

O. Akanyeti^{1,2}, Joy Putney^{1,3}, Y.R. Yanagitsuru¹, G.V. Lauder⁴, W.J. Stewart^{1,5}, J.C. Liao¹

¹ The Whitney Laboratory for Marine Bioscience, Department of Biology, University of Florida,
St. Augustine, FL 32080, USA.

² The Department of Computer Science, Aberystwyth University, Ceredigion, SY23 3FL, Wales.

³ The School of Biological Sciences, Georgia Institute of Technology, Atlanta, GA 30332, USA.

⁴ The Department of Organismic and Evolutionary Biology, Harvard University, Cambridge, MA
02138, USA.

⁵ The Department of Science, Eastern Florida State College, Melbourne, FL 32935, USA.

Author for correspondence: J.C.L. (jliao@whitney.ufl.edu), O.A. (ota1@aber.ac.uk)

Abstract

Swimming animals need to generate propulsive force to overcome drag, regardless of whether they swim steadily or accelerate forward. While locomotion strategies for steady swimming are well characterized, far less is known about acceleration. Animals exhibit many different ways to swim steadily, but we show here that this behavioral diversity collapses into a single swimming pattern during acceleration regardless of the body size, morphology, and ecology of the animal. We draw on the fields of biomechanics, fluid dynamics and robotics to demonstrate that there is a fundamental difference between steady swimming and forward acceleration. We provide empirical evidence that the tail of accelerating fishes can increase propulsive efficiency by enhancing thrust through the alteration of vortex ring geometry. Our study provides new insight into how propulsion can be altered without increasing vortex ring size, and represents a fundamental departure from our current understanding of the hydrodynamic mechanisms of acceleration. Our findings reveal a unifying hydrodynamic principle that is likely conserved in all aquatic, undulatory vertebrates.

45 **Significance Statement**

46 The ability to move is one of the key evolutionary events that led to the complexity of vertebrate
47 life. The most speciose group of vertebrates, fishes, displays an enormous variation of movement
48 patterns during steady swimming. We discovered that this behavioral diversity collapses into one
49 movement pattern when fishes are challenged to increase their swimming speed, regardless of
50 their body size, shape and ecology. Using flow visualization and biomimetic models, we
51 provide the first mechanistic understanding of how this conserved movement pattern allows
52 fishes to accelerate quickly.

53 \body

54

Introduction

Over the course of evolutionary time, patterns of animal locomotion have diversified to take advantage of the physical environment through the interplay of morphology, physiology and neural control. Yet, two fundamental principles of locomotion in most animals remain the same: 1) Force is generated by transferring momentum to the environment through repetitive motions such as body undulations and oscillating appendages (legs, fins, or wings), and 2) the locomotor speed is modulated by controlling the amplitude and frequency of these periodic motions (1, 2). Previous studies have demonstrated that the degrees of freedom in amplitude and frequency control are not limitless, but rather constrained by the physical laws imposed by the environment. For example, flying animals must maintain a high wing-beat frequency to generate enough lift, controlling speed primarily by altering the wing's angle of attack(3). In contrast, the morphology and locomotion strategies of aquatic animals have adapted to moving through a viscous environment where gravitational forces are negligible. Among these strategies, the ancestral state of aquatic locomotion is axial undulation, where muscle contractions bend the body into a mechanical wave that passes from head to tail (4). The interaction of angled body surfaces with the surrounding fluid propels the animal forward, and the movements of the entire body contribute to the overall swimming performance (5-10).

Over the past several decades, a number of studies have investigated the kinematics (11-14), muscle activity (15-18) and hydrodynamics (19-21) of tail movements, in particular how tail beat amplitude and frequency are controlled during steady swimming. Most undulatory vertebrates such as fishes, alligators, dolphins and manatees control speed by primarily modulating tail beat frequency while maintaining a relatively low tail beat amplitude (22-25). At high steady swimming speeds, tail beat amplitude reaches a plateau at around 0.2 body length

(L). Computational studies (26-29) and experiments with hydrofoils (30, 31) suggest that swimming animals operate in this range to maintain high swimming efficiency.

How do these mechanisms apply when a steadily-swimming animal accelerates forward, which is often used to catch prey, avoid predators or save energy during migrations (32, 33)? One hypothesis is that speed is gained only by further increasing the tail beat frequency (34-37). Alternatively, an animal can bend its body maximally to accelerate large amounts of fluid, as seen in Mauthner initiated C-starts (38-41). Yet emerging studies suggest that forward acceleration exhibits distinct kinematics (42-46) that defy both hypotheses, indicating that acceleration may have its own optimization strategy. Although forward acceleration has been a topic of interest for decades in the field of aquatic locomotion (39, 43), a comprehensive understanding of its prevalence and underlying mechanisms has remained elusive. Here, we identify a new undulatory locomotion strategy for forward acceleration by integrating complementary approaches: biological experiments with live fishes and physical experiments with bio-mimetic fish models.

Results and Discussion

Acceleration kinematics across fish phylogeny

We discovered that in fishes tail beat amplitude is consistently higher during acceleration than during steady swimming (Fig. 1). This pattern is conserved across 51 species examined, with representatives from a wide range of phylogenetic positions from chondrichthyes (e.g. bonnethead shark, *Sphyrna tiburo*) to tetraodontiformes (e.g. striped burrfish, *Chilomycterus schoepfi*). These species exhibit vastly different body shapes, ecological habitats and swimming modes (Table S1). Some species use median or pectoral fins during steady swimming (e.g. clown knifefish, *Chitala ornata* and sergeant major, *Abudefduf saxatilis*), but always revert to body undulation when they accelerate forward from steady swimming.

When we plot tail beat amplitude during acceleration against steady swimming for all species, we found that the relationship is linear (Fig. S1a). This suggests that the relative increase in tail beat amplitude during acceleration is constant at $34\pm4\%$. However, there is substantial variation in the absolute amplitude values that depends on body length and shape. For example, when body length is held constant, elongate fishes such as Florida gar (*Lepisosteus platyrhincus*) and Northern barracuda (*Sphyraena borealis*) accelerate with lower tail beat amplitudes ($0.19\pm0.01 L$) compared to more fusiform fishes such as tarpon and red drum ($0.24\pm0.01 L$). We also found that during acceleration tail beat amplitude decreases with body length (Fig. S1b).

To better understand if there is a common propulsive strategy across fish diversity, we next performed a more detailed midline analysis of the entire body during steady swimming and forward acceleration for 9 species. Despite extreme differences in body shape and swimming mode, we found that all fishes share similar midline acceleration kinematics. These acceleration bouts are usually brief, typically less than five tail beats. All points along the body show higher

amplitudes compared to steady swimming, but not as high as seen during C-starts (39, 40) (Fig. S2-4). Further analyses on the travelling body wave and tail movement suggest efficient force production during acceleration (Table S2). The average values across 10 species for slip ratio, Strouhal number (St) and maximum angle of attack (α_{max}) are 0.80 ± 0.02 , 0.41 ± 0.01 , and $22.71 \pm 0.65^\circ$, respectively. Slip ratios approaching 1 reveal high swimming efficiency, while experiments with thrust-producing, harmonically oscillating foils show that propulsive efficiency is maximized when St falls within the range of 0.2 and 0.5 and α_{max} is between 15° and 25° (30).

In addition to the species studied here, similar acceleration kinematics was previously observed in American eels (44). These elevated amplitudes are most notable around the head and tail. The onset of acceleration (which can be easily recognized because of strong head yaw and a faster tail beat) provides a reference point to interpret the phase relationship between head and tail. By doing so, we found that the motion of the head always precedes the motion of the tail, indicating that the body wave is initiated by strong head movements in all species, though the timing between head and tail movements is not constant. To more closely investigate the kinematics and hydrodynamics of acceleration, we chose a generalized teleost fish, the rainbow trout (*Oncorhynchus mykiss*). The swimming kinematics of this species has been studied in great detail for steady swimming and other behaviors but not for acceleration (5, 13, 47-54). Like other species tested in this study, the body amplitudes of trout are higher during acceleration than during steady swimming (Fig. S5a), and head movements precede the motion of the tail (Fig. S5b).

We next examined how swimming speed and acceleration depend on tail beat amplitude, given that a range of amplitudes is evident for each behavior (Fig. S5c). As others have shown previously (44), we found that in general tail beat frequency, not tail beat amplitude, has the

most effect during both behaviors (Fig. S5d). Multiple regression analysis revealed that steady swimming speed increases only with tail beat frequency. This trend is similar during acceleration, though tail beat amplitude also has a minor effect (Table S3). Our results suggest that tail beat amplitude does not change during steady swimming or acceleration, but jumps discretely by ~30% when fish transition from one behavior to another. Thus, trout appear to have two undulatory gears based on tail beat amplitude; one for steady swimming and another for acceleration. Our results suggest that this discrete jump in tail beat amplitude during acceleration is correlated with increased head yaw (Fig. S5e), and these movements are tightly phase-locked, with the head preceding the tail (Fig. S5f).

Hydrodynamic effects of increased tail beat amplitude during acceleration

We next investigated how increased tail beat amplitude relates to thrust production and propulsive efficiency by using a combination of quantitative flow visualization experiments on live fish and experiments with actuated, soft-bodied robotic models. Results from particle image velocimetry show that fish can reach a maximum acceleration rate of $20 L s^{-2}$ from initial swimming speed of $3 L s^{-1}$. To accomplish this, fish transfer more axial momentum to the fluid by generating stronger vortices compared to steadily swimming fish (Fig. 2a). Similar wake structures were previously observed in zebrafish (55), eel (44) and carp (45). In addition, fish entrain more fluid around their posterior body to strengthen shed vortices (Fig. 2b). This occurs because the posterior body has a greater curvature, which creates a low pressure region in the concavity (Fig. 2b, $t=12.5$ ms). The entrained fluid in this low pressure region (blue) follows the traveling body wave until it reaches the trailing edge of the tail ($t=50$ ms). At the point when the tail reverses direction, the fluid starts to roll off the tail and into the wake ($t=56.3$ ms).

Concurrently, the body concavity causes flow to build up on the opposite side. This fluid (red) starts getting released to the wake as the tail increases its velocity ($t = 68.8$ ms). When the tail reaches its maximum velocity a vortex is formed ($t=81.3$ ms), owing to the occurrence of two bodies of fluid moving in opposite directions. Our results indicate that during acceleration body undulations of trout are responsible for increased wake velocity and vorticity. This is not surprising as multiple studies have shown that body-induced flows can enhance vortex shedding in other species (7, 8, 10, 19, 56, 57).

When fish swim, they generate vortex rings (58-60). We see this in two dimensions as two counter-rotating vortices (i.e. vortex cores) in the wake after each tail beat (61-63). In recent years, estimating locomotive forces from wake measurements has garnered much interest with hopes of better understanding the resultant motion of the animal (41, 56, 64-66). Several methods have been proposed to estimate locomotive forces (56, 64, 67, 68). The one which we used in this study is based on the classical vortex ring theory (69). We calculated the impulse (i.e. the average force) applied to the fluid during each tail beat by measuring the circulation, jet angle (θ), core diameter (D_o) and the spacing between the two vortex cores (D). We found that an accelerating trout generates an impulse (along the swimming direction) that is at least 4 times higher than that required for its initial steady swimming speed (Fig. 2c). This higher impulse is due to $172 \pm 16\%$ increase in vorticity. In addition, the jet angle is oriented $\sim 30 \pm 3\%$ more downstream, which devotes a greater proportion of the impulse along the swimming direction.

We found that D is reduced by $\sim 25\%$ from $0.33 L$ to $0.25 L$ when fish transition from steady swimming to acceleration. At first glance this may be surprising given that the impulse and kinetic energy of a ring is proportional to its size. However, impulse and energy also depend on the geometry of the vortex ring itself. One key parameter of the ring geometry is the ratio

between minor and major axis diameters (d/D). When d/D approaches one, the ring becomes more axisymmetric, which is favorable because axisymmetric rings possess the maximum amount of energy relative to other shapes that maintain the same total impulse (70, 71). Given that d is always constrained by the span of the tail (7, 58, 59, 62, 72), the axisymmetry of the ring primarily depends on D . Our results show that during steady swimming trout generate elliptical rings ($d/D=0.66$). In contrast, we found that during acceleration the geometry of the vortex rings become more axisymmetric ($d/D=0.88$).

The impulse of a vortex ring is also proportional to the ratio of its core diameter to its ring diameter (D_o/D). In addition to having a more axisymmetric shape, we found that the vortex rings generated by accelerating trout have thicker cores ($D_o/D=0.37\pm0.02$) than those generated by trout swimming steadily ($D_o/D=0.25\pm0.01$). It has been shown that for vortex rings generated by a piston pushing a cylinder of fluid through a nozzle there is a limit in generating thicker arms efficiently, because at some point (piston stroke to diameter ratio >3.5) separation occurs and energy dissipated by a trailing edge of fluid (73-75). For finite-core, axisymmetric vortex rings which propagate steadily (76), this piston stroke to diameter ratio corresponds to $D_o/D = 0.42$ in a vortex ring (77, 78). Perhaps not coincidentally, the vortex rings generated by accelerating trout have D_o/D close to 0.42. In order to evaluate whether our fish-generated vortex rings during acceleration can be compared to nozzle-generated rings, we analyzed their velocity and vorticity distributions along a center line connecting the two vortex cores, and confirmed that they closely match the values reported for nozzle-generated rings (73, 79) (Fig. S6a-c). In addition, we investigated the temporal dynamics of vortex rings once they are shed into the wake, and found that they translate downstream with a constant velocity while preserving their D_o/D ratio (Fig.

S6d). What this suggests is that the hydrodynamic principles of efficient thrust production in oscillating fish may be similar to those observed during biological jet propulsion (65, 80-82).

Overall, our findings indicate that accelerating trout generate more thrust, not by generating larger rings but, by modulating their geometry and orientation. To investigate how common this phenomenon is, we analyzed d/D , D_o/D and θ of four additional species with different swimming modes and body shapes and found similar results (Table S3). In addition, flow imaging on a similar sized American eel ($L=23$ cm) shows that during acceleration anguilliform swimmers also generate vortex rings with comparable D_o/D ratio (~ 0.4 based on Fig. 1b in (44)). It remains to be seen, however, how D_o/D ratio scales with body size, given that it is significantly higher (0.6-0.7) for smaller fish such as zebrafish (83) and koi carps (45). [Note that a 2-dimensional geometric analysis of vortex rings provides an initial, albeit qualitative understanding on how fishes accelerate efficiently. Concatenated, ring-like structures involved in the wakes of fishes can be highly elongated and 3-dimensional, and may not have the same properties \(e.g. momentum, energy, and stability\) as nozzle-generated rings.](#)

Relationship between tail kinematics and vortex ring geometry We next propose a set of equations to provide a mechanistic understanding of how the geometry (d/D and D_o/D) and angle (θ) of a vortex ring depend on the tail kinematics. Because the oscillating tail generates each core of a vortex ring successively, we used trigonometric relations to define $D = \sqrt{a^2 + b^2}$ and $\theta = \tan^{-1}\left(\frac{a}{b}\right)$, where a and b are the vertical and horizontal spacing between the two cores, respectively. Based on our wake analysis, the vertical spacing depends on the tail beat amplitude (i.e. a = half of the tail beat amplitude), and the horizontal spacing depends on the tail beat frequency and swimming speed (i.e. b = swimming speed multiplied by half tail beat cycle). To

validate our approach, we calculated D and θ for trout swimming steadily at $3 L s^{-1}$ and accelerating from the same initial speed. During acceleration we assumed that the swimming speed was $4 L s^{-1}$ (i.e. the average between initial and final swimming speeds). We compared the predicted D and θ to those measured experimentally, and found a good match (Fig. 2D, $D=0.31 L$ and $\theta=75.07^\circ$ during steady swimming and $D=0.22 L$ and $\theta=63.43^\circ$ during acceleration).

Once we validated our approach, we used it to further investigate the contribution of increased tail beat amplitude during acceleration. We computationally explored an alternative scenario where the tail beat amplitude was kept constant at the value observed for steady swimming ($0.16 L$), and speed was gained by further increasing the tail beat frequency (i.e. hypothetical acceleration). Given that thrust is proportional to the square of tail beat frequency multiplied by the square of tail beat amplitude (84, 85), we increased the tail beat frequency from 10 Hz to 12.5 Hz in order to maintain the same effective thrust. We found that this had no effect on the ring angle ($\theta=63.43^\circ$), but generated a suboptimal $D=0.18 L$ with $d/D=1.22$ and $D_o/D=0.56$ (we assumed that $d=0.22 L$ and $D_o=0.1 L$). Therefore, we believe that the increase in tail beat amplitude observed in trout is the key to geometrically generating the most efficient rings.

The swimming performance of robotic models increases with tail beat amplitude

While it is favorable to generate more thrust by producing vortex rings with optimal geometry, this does not reveal the overall swimming efficiency of an accelerating fish because motions that produce them may be costly. It is not unreasonable to imagine that large lateral body amplitudes would incur large drag penalties (44, 45). To resolve this tradeoff, we employed experiments with a biomimetic trout model to systematically explore how different tail beat amplitudes affect steady swimming and acceleration performance (Fig S7). This level of

experimental control is impossible to achieve with live fish. We generated undulatory movements in our flexible fish model from a single actuation point located just posterior to the head. Therefore, we were able to control tail beat amplitude by modulating the head yaw.

We first measured performance during steady swimming and acceleration at yaw amplitudes very similar to those of live fish (10° and 20°). We found that during steady swimming the model performed better when it is actuated with smaller yaw (Fig. S8a). However, during acceleration this relationship is reversed; swimming performance is consistently higher with larger yaw (Fig. S8b). This suggests that there is no convergence of optimum head yaw between steady swimming and acceleration. While steady swimming seeks to preserve momentum by streamlining motions, during acceleration additional momentum must be generated despite drag costs.

To determine if there are yaw values that maximize swimming efficiency during acceleration, we measured efficiency at yaw amplitudes between 0° and 30° at 3° increments. We found that efficiency increases linearly with yaw amplitudes up to 20° , beyond which values plateau (Fig. 3). When we map head yaw from live fish onto our model performance curve, we found that increasing head yaw from steady swimming values to acceleration values can create an increase in efficiency up to 100%. It is perhaps no accident that the yaw amplitudes chosen by accelerating fish fall within the range that gives greatly increased propulsive efficiency compared to steady swimming. We hypothesize that this is due to generating hydrodynamically more efficient vortex rings, based on our flow measurements in the wake of live fishes. However, increasing head yaw to accelerate with more optimal vortex rings does not mean that producing these rings costs less than the rings produced during steady swimming (Figure S9 shows a 50% increase in mechanical power input for increased head yaw).

279 The ability to move is one of the key evolutionary events that led to the diversity and
280 complexity of vertebrate life. Given that movement through fluids is energetically costly, fishes
281 have found many ways to minimize drag during normal, steady swimming, such as keeping the
282 body straight and using median or paired fin locomotion (86-88). While steady swimming is
283 optimized for endurance by minimizing the energetic investment, acceleration favors
284 maximizing force production to escape quickly from predators or capture elusive prey. Here, we
285 show that the enormous behavioral diversity observed during steady swimming collapses into a
286 single locomotion strategy when fishes transition to forward acceleration. We believe that this
287 strategy is likely conserved across all undulatory swimmers and not just fishes because it is
288 hydrodynamically the optimal solution to maximize propulsive efficiency.

Methods

All research protocols were approved by the Institutional Animal Care and Use Committee at the University of Florida. All data analyses were performed in Matlab (Mathworks) and all values are shown as mean \pm standard error of the mean, unless stated otherwise.

Diversity of swimming kinematics across species Our data set included 51 species of salt and freshwater fish (105 individuals, from 20 taxonomic orders), which were either obtained from commercial dealers or wild caught using cast net or hook-and-line. The details about these species are given in Table S1, and [the research protocols are described in Text S1](#).

Swimming hydrodynamics of rainbow trout We used digital particle image velocimetry to quantify the flow fields around and behind steady swimming and accelerating trout. We estimated wake forces as described in (66) (see [Text S2](#) for more details on the experimental procedures and data analysis).

Experiments with the physical fish model We performed the experiments in the flow tank at Harvard University which is customized to house a computer-controlled external actuator. We used this system in the past to evaluate the swimming performance in a number of swimming mechanical models (5, 89-91). Here, we systematically moved the physical model with different tail kinematics and measured the total sum of forces acting on the whole body. For these

311 measurements, we calculated the propulsive force produced by the model and the corresponding
312 power output of the actuator as described in (92) ([see Text S3 for more details](#)).

Acknowledgements

We thank Sefki Kolozali for his comments on the earlier version of the manuscript. We thank Mikhaila Marecki and Elias Lunsford for helping to conduct fish experiments and to digitize fish midlines. We also thank Ashley N. Peterson and Patrick J.M. Thornycroft for helping to design and fabricate fish models and conduct experiments with them. Wild caught species were collected with the generous assistance of Craig Barzso, Jessica Long, Adam Pacetti and John Perkner. This work was supported by ONR N00014-0910352 to G.V.L., Research Coordination Network Travel grant DBI-RCN 1062052 to O.A. and J.C.L., National Institute on Deafness and Other Communication Disorders grant RO1-DC-010809 and National Science Foundation grant IOS 1257150 to J.C.L.

323 **References**

- 324 1. Alexander RM (2003) *Principles of Animal Locomotion* (Princeton University Press).
- 325 2. Biewener (2003) *Animal Locomotion* (Oxford University Press).
- 326 3. Nudds RL, Taylor GK, & Thomas ALR (2004) Tuning of Strouhal number for high propulsive
327 efficiency accurately predicts how wingbeat frequency and stroke amplitude relate and scale with
328 size and flight speed in birds. *Proceedings Royal Society London B* 271:2071-2076.
- 329 4. Gray J (1953) The locomotion of fishes. *Essays in Marine Biology*, eds Marshall SM & Orr AP
330 (Oliver and Boyd, Edinburgh), pp 1-16.
- 331 5. Akanyeti O, *et al.* (2016) Fish optimize sensing and respiration during undulatory swimming.
332 *Nature Communications* 7.
- 333 6. Gemmell BJ, Collin SP, Costello JH, & Dabiri JO (2015) Suction-based on propulsion as a
334 basis for efficient animal swimming. *Nature communications* 6(8790).
- 335 7. Kern S & Koumoutsakos P (2006) Simulations of optimized anguilliform swimming. *The*
336 *Journal of Experimental Biology* 209:4841-4857.
- 337 8. Müller UK, Smit J, Stamhuis EJ, & Videler JJ (2001) How the body contributes to the wake in
338 undulatory fish swimming: flow fields of a swimming eel (*Anguilla anguilla*). *The Journal of*
339 *Experimental Biology* 204:2751-2762.
- 340 9. Nauen JC & Lauder GV (2001) Three-dimensional analysis of finlet kinematics in the chub
341 mackerel (*Scomber japonicus*). *The Biological Bulletin* 200(1):9-19.
- 342 10. Borazjani I & Sotiropoulos F (2009) Numerical investigation of the hydrodynamics of
343 anguilliform swimming in the transitional and inertial flow regimes. *Journal of Experimental*
344 *Biology* 212:576-592.
- 345 11. Bainbridge R (1958) The speed of swimming of fish as related to size and to the frequency
346 and amplitude of the tail beat. *The Journal of Experimental Biology* 35:109-133.
- 347 12. Videler JJ & Hess F (1984) Fast continuous swimming of two pelagic predators, saithe
348 (*Pollachius virens*) and mackerel (*Scomber scombrus*): a kinematic analysis. *The Journal of*
349 *Experimental Biology* 109:209-228.
- 350 13. Webb PW, Kostecki PT, & Stevens ED (1984) The effect of size and swimming speed on the
351 locomotor kinematics of rainbow trout. *The Journal of Experimental Biology* 109:77-95.
- 352 14. Jayne BC & Lauder GV (1995) Speed Effects on Midline Kinematics During Steady
353 Undulatory Swimming of Largemouth Bass, *Micropterus salmoides*. *The Journal of*
354 *Experimental Biology* 198(2):585-602.
- 355 15. Rome LC, Swank D, & Corda D (1993) How fish power swimming. *Science* 261:340-343.
- 356 16. Jayne BC & Lauder GV (1996) New data on axial locomotion in fishes: how speed affects
357 diversity of kinematics and motor patterns. *American Zoologist* 36(6):642-655.
- 358 17. Altringham J & Ellerby DJ (1999) Fish swimming: patterns in muscle function. *The Journal*
359 *of Experimental Biology* 202(Pt 23):3397-3403.
- 360 18. Coughlin DJ (2002) Aerobic muscle function during steady swimming in fish. *Fish and*
361 *Fisheries* 3:63-78.
- 362 19. Videler JJ, Müller UK, & Stamhuis EJ (1999) Aquatic vertebrate locomotion: Wakes from
363 body waves. *The Journal of Experimental Biology* 202(23):3423-3430.
- 364 20. Drucker EG & Lauder GV (2002) Experimental Hydrodynamics of Fish Locomotion:
365 Functional Insights from Wake Visualization. *Integrative and Comparative Biology* 42(2):243-
366 257.

- 21.Lauder GV & Tytell ED (2005) Hydrodynamics of Undulatory Propulsion. *Fish Physiology*, (Academic Press), Vol Volume 23, pp 425-468.
- 22.Bainbridge R (1963) Caudal fin and body movements in the propulsion of some fish. *The Journal of Experimental Biology* 40:23-56.
- 23.Fish FE (1984) Kinematics of Undulatory Swimming in the American Alligator. *American Society of Ichthyologists and Herpetologists* 4:839-843.
- 24.Fish FE (1998) Comparative kinematics and hydrodynamics of odontocete cetaceans: morphological and ecological correlates with swimming performance. *Journal of Experimental Biology* 201:2867-2877.
- 25.Kojaszewski T & Fish FE (2007) Swimming kinematics of the Florida manatee (*Trichechus manatus latirostris*): hydrodynamic analysis of an undulatory mammalian swimmer. *Journal of Experimental Biology* 210:2411-2418.
- 26.Eloy C (2013) On the best design for undulatory swimming. *Journal of Fluid Mechanics* 717:48-89.
- 27.Schultz WW & Webb PW (2002) Power Requirements of Swimming: Do New Methods Resolve Old Questions? *Integrative and Comparative Biology* 42:1018-1025.
- 28.van Rees WM, Gazzola M, & Koumoutsakos P (2015) Optimal morphokinematics for undulatory swimmers at intermediate Reynolds numbers. *Journal of Fluid Mechanics* 775:178-188.
- 29.Tytell ED, Hsu C-Y, Williams TL, Cohen AH, & Fauci LJ (2010) Interactions between internal forces, body stiffness, and fluid environment in a neuromechanical model of lamprey swimming. *National Academy of Sciences* 107(46):19832–19837.
- 30.Anderson JM, Streitlien K, Barrett DS, & Triantafyllou MS (1998) Oscillating foils of high propulsive efficiency. *Journal of Fluid Mechanics* 360:41-72.
- 31.Taylor GK, Nudds RL, & Thomas AL (2003) Flying and swimming animals cruise at a Strouhal number tuned for high power efficiency. *Nature* 425(6959):707-711.
- 32.Weihs D & Webb PW (1983) Optimization of Locomotion. *Fish Biomechanics*, eds Webb PW & Weihs D (Praeger Publishers, New York).
- 33.Gleiss AC, *et al.* (2011) Convergent evolution in locomotory patterns of flying and swimming animals. *Nature Communications* 2.
- 34.Rome LC, *et al.* (1988) Why animals have different muscle fibre types. *Nature* 335:824 - 827.
- 35.Johnson TP, Syme DA, Jayne BC, Lauder GV, & Bennett AF (1994) Modeling red muscle power output during steady and unsteady swimming in largemouth bass. *American Journal of Physiology- Regulatory, Integrative and Comparative Physiology* 267(2 pt 2):R481-R488.
- 36.Weihs D (1974) Energetic Advantages of Burst Swimming of Fish. *Journal of Theoretical Biology* 48:215-229.
- 37.Videler JJ & Weihs D (1982) Energetic advantages of burst-and-coast swimming of fish at high speeds. *Journal of Experimental Biology* 97:169-178.
- 38.Eaton RC, Bombardieri RA, & Meyer DL (1977) The Mauthner-initiated startle response in teleost fish. *Journal of Experimental Biology* 66(1):65-81.
- 39.Domenici P & Blake RW (1997) The Kinematics and Performance of Fish Fast-Start Swimming. *The Journal of Experimental Biology* 200(pt 8):1165-1178.
- 40.Wakeling JM (2006) Fast-start mechanics. *Fish Biomechanics*, eds Shadwick RE & Lauder GV (Academic Press, San Diego), pp 333-368.
- 41.Tytell ED & Lauder GV (2008) Hydrodynamics of the escape response in bluegill sunfish, *Lepomis macrochirus*. *Journal of Experimental Biology* 211:3359-3369.

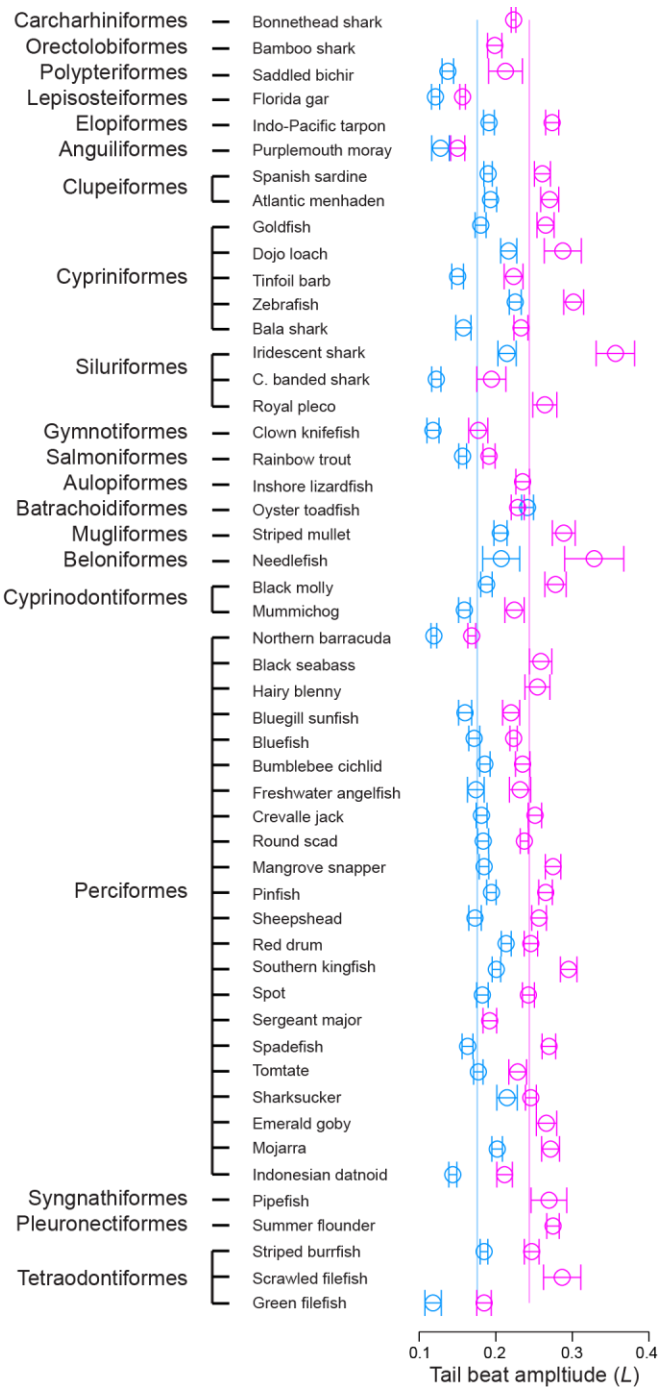
42. Fierstine HL & Walters V (1968) Studies in locomotion and anatomy of scombroid fishes. *Memoirs of the Southern California Academy of Science* 6:1-31.
43. Videler JJ (1993) *Fish Swimming* (Chapman and Hall, New York).
44. Tytell ED (2004) Kinematics and hydrodynamics of linear acceleration in eels, *Anguilla rostrata*. *Philosophical Transactions Royal Society London B* 271:2535-2540.
45. Wu G, Yang Y, & Zeng L (2007) Kinematics, hydrodynamics and energetic advantages of burst-and-coast swimming of koi carps (*Cyprinus carpio koi*). *Journal of Experimental Biology* 210:2181-2191.
46. van Leeuwen JL, Lankheet MJM, Akster HJ, & Osse JWM (1990) Function of red axial muscles of carp (*Cyprinus carpio* L.): recruitment and normalized power output during swimming in different modes. *Journal of Zoology London* 220(123-145).
47. Drucker EG & Lauder GV (2003) Function of pectoral fins in rainbow trout: behavioral repertoire and hydrodynamic forces. *Journal of Experimental Biology* 206(Pt 5):813-826.
48. Drucker EG & Lauder GV (2005) Locomotor function of the dorsal fin in rainbow trout: kinematic patterns and hydrodynamic forces. *The Journal of Experimental Biology* 208(Pt 23):4479-4494.
49. Coughlin DJ (2000) Power production during steady swimming in largemouth bass and rainbow trout. *The Journal of Experimental Biology* 203:617-629.
50. Ellerby DJ & Altringham JD (2001) Spatial variation in fast muscle function of the rainbow trout *Oncorhynchus mykiss* during fast-starts and sprinting. *The Journal of Experimental Biology* 204(Pt 13):2239-2250.
51. Liao JC, Beal DN, Lauder GV, & Triantafyllou MS (2003) The Kármán gait: novel body kinematics of rainbow trout swimming in a vortex street. *The Journal of Experimental Biology* 206(6):1059-1073.
52. Akanyeti O & Liao JC (2013) Effect of flow speed and body size on Kármán gait kinematics in rainbow trout. *The Journal of Experimental Biology* 216:3442-3449.
53. Stewart WJ, Tian F, Akanyeti O, Walker CJ, & Liao JC (2016) Refuging rainbow trout selectively exploit flows behind tandem cylinders. *Journal of Experimental Biology* 219(14):2182-2191.
54. Akanyeti O & Liao JC (2013) A kinematic model of Kármán gaits in rainbow trout. *The Journal of Experimental Biology* 216(24):4666-4677.
55. Müller UK, Stamhuis EJ, & Videler JJ (2000) Hydrodynamics of unsteady fish swimming and the effects of body size: Comparing the flow fields of fish larvae and adults. *The Journal of Experimental Biology* 203(2):193-206.
56. Tytell ED & Lauder GV (2004) The hydrodynamics of eel swimming: I. Wake structure *Journal of Experimental Biology* 207:1825-1841.
57. Gemmell BJ, *et al.* (2016) How the bending kinematics of swimming lampreys build negative pressure fields for suction thrust. *Journal of Experimental Biology* 219:3884-3895.
58. Flammang BE, Lauder GV, Troolin DR, & Strand TE (2011) Volumetric imaging of fish locomotion. *Biology Letters* 7(5):695-698.
59. Mendelson L & Techet AH (2015) Quantitative wake analysis of a freely swimming fish using 3D synthetic aperture PIV. *Experiments in Fluids* 56(135):1-19.
60. Tytell ED, Standen EM, & Lauder GV (2008) Escaping Flatland: three dimensional kinematics and hydrodynamics of median fins in fishes. *Journal of Experimental Biology* 211(2):187-195.

61. Blickhan R, Krick C, Zehren D, Nachtigall W, & Breithaupt T (1992) Generation of a vortex chain in the wake of a Subundulatory swimmer. *Naturwissenschaften* 79(5):220-221.
62. Nauen JC & Lauder GV (2002) Hydrodynamics of caudal fin locomotion by chub mackerel, *Scomber japonicus* (Scombridae). *The Journal of Experimental Biology* 205(12):1709-1724.
63. Müller UK, Van den Heuvel BLE, Stamhuis EJ, & Videler JJ (1997) Fish foot prints: morphology and energetics of the wake behind a continuously swimming mullet (*Chelon labrosus* Risso). *The Journal of Experimental Biology* 200(22):2893-2906.
64. Drucker EG & Lauder GV (1999) Locomotor forces on a swimming fish: three-dimensional vortex wake dynamics quantified using digital particle image velocimetry. *Journal of Experimental Biology* 202(Pt 18):2393-2412.
65. Bartol IK, Krueger PS, Stewart WJ, & Thompson JT (2009) Hydrodynamics of pulsed jetting in juvenile and adult brief squid *Loligo brevis*: evidence of multiple jet 'modes' and their implication of propulsive efficiency. *Journal of Experimental Biology* 212:1889-1903.
66. Epps BP & Techet AH (2007) Impulse generated during unsteady maneuvering of swimming fish. *Experiments in Fluids* 43:691-700.
67. Noca F, Shiels D, & Jeon D (1999) A comparison of methods for evaluating time-dependent fluid dynamic forces on bodies, using only velocity fields and their derivatives. *Journal of Fluids and Structures* 13:551-578.
68. Dabiri JO (2005) On the estimation of swimming and flying forces from wake measurements. *Journal of Experimental Biology* 208:3519-3532.
69. Batchelor GK (2000) *An Introduction to Fluid Dynamics* (Cambridge University Press).
70. Kelvin L (1880) Vortex statistics. *Philosophical Magazine* 10:97-109.
71. Dabiri JO (2009) Optimal vortex formation as a unifying principle in biological propulsion. *Annual Review of Fluid Mechanics* 41:17-33.
72. Borazjani I & Daghooghi M (2013) The fish tail motion forms an attached leading edge vortex. *The Royal Society Proceedings B* 280(1756):20122071.
73. Gharib M, Rambod E, & Shariff K (1998) A universal time scale for vortex ring formation. *Journal of Fluid Mechanics* 360:121-140.
74. Krueger PS & Gharib M (2005) Thrust augmentation and vortex ring evolution in a fully pulsed jet. *The Journal of American Institute of Aeronautics and Astronautics* 43(4):792-801.
75. Mohseni K & Gharib M (1998) A model for universal time scale of vortex ring formation. *Physics of Fluids* 10:2436-2438.
76. Norbury J (1973) Family of steady vortex rings. *Journal of Fluid Mechanics* 57:417-431.
77. Linden PF & Turner JS (2004) 'Optimal' vortex rings and aquatic propulsion mechanisms. *Proceedings of The Royal Society B* 271(1539):647-653.
78. Linden PF & Turner JS (2001) The formation of 'optimal' vortex rings, and the efficiency of propulsion devices. *Journal of Fluid Mechanics* 427:61-72.
79. Weigand A & Gharib M (1997) On the evolution of laminar vortex rings. *Experiments in Fluids* 22:447-457.
80. Dabiri JO, Collin SP, Katija K, & Costello JH (2010) A wake-base correlate of swimming performance and foraging behavior in seven co-occurring jellyfish species. *Journal of Experimental Biology* 213:1217-1225.
81. Gharib M, Rambod E, Kheradvar A, Sahn DJ, & Dabiri JO (2006) Optimal vortex formation as an index of cardiac health. *Proceedings of the National Academy of Sciences of the United States of America* 103:6305-6308.

- 82.Dabiri JO, Collin SP, & Costello JH (2006) Fast-swimming hydromedusae exploit velar kinematics to form an optimal vortex wake. *Journal of Experimental Biology* 209:2025-2033.
- 83.Müller UK & van Leeuwen JL (2004) Swimming of larval zebrafish: ontogeny of body waves and implications for locomotory development. *The Journal of Experimental Biology* 207(Pt 5):853-868.
- 84.Wu TY (1977) Introduction to scaling of aquatic animal locomotion. *Scale Effects of Animal Locomotion*, ed Pedley TJ (Academic Press, New York, NY), pp 203-232.
- 85.Lighthill J (1971) Large-amplitude elongated body theory of fish locomotion. *Proceedings of the Royal Society B: Biological Sciences* 179(1055):125-138.
- 86.Lighthill J (1993) Estimates of Pressure Differences across the Head of a Swimming Clupeid Fish. *Philosophical Transactions of the Royal Society B: Biological Sciences* 341(1296):12.
- 87.Webb PW (1992) Is the high cost of body/caudal fin undulatory swimming due to increased friction drag or inertial recoil? *The Journal of Experimental Biology* 162:157-166.
- 88.Fish FE (1998) Imaginative solutions by marine organisms for drag reduction. *Proceedings of the International Symposium on Seawater Drag Reduction*:443-450.
- 89.Lauder GV, Flammang BE, & Alben S (2012) Passive robotic models of propulsion by the bodies and caudal fins of fish. *Integrative and Comparative Biology* 52:576-587.
- 90.Shelton RM, Thornycroft JMP, & Lauder VG (2014) Undulatory locomotion of flexible foils as biomimetic models for understanding fish propulsion. *Journal of Experimental Biology* 217:2110-2120.
- 91.Lauder GV & Tangorra JL (2015) Fish locomotion: biology and robotics of body and fin-based movements. *Robot Fish - Bioinspired Fishlike Underwater Robots*, eds Du R, Li Z, Youcef-Toumi K, & Valdivia Y Alvarado P (Springer-Verlag, Berlin), pp 25-49.
- 92.Read DA, Hover FS, & Triantafyllou MS (2003) Forces on oscillating foils for propulsion and maneuvering. *Journal of Fluids and Structures* 17:163-183.

532 **Figures**

533 **Figure 1**

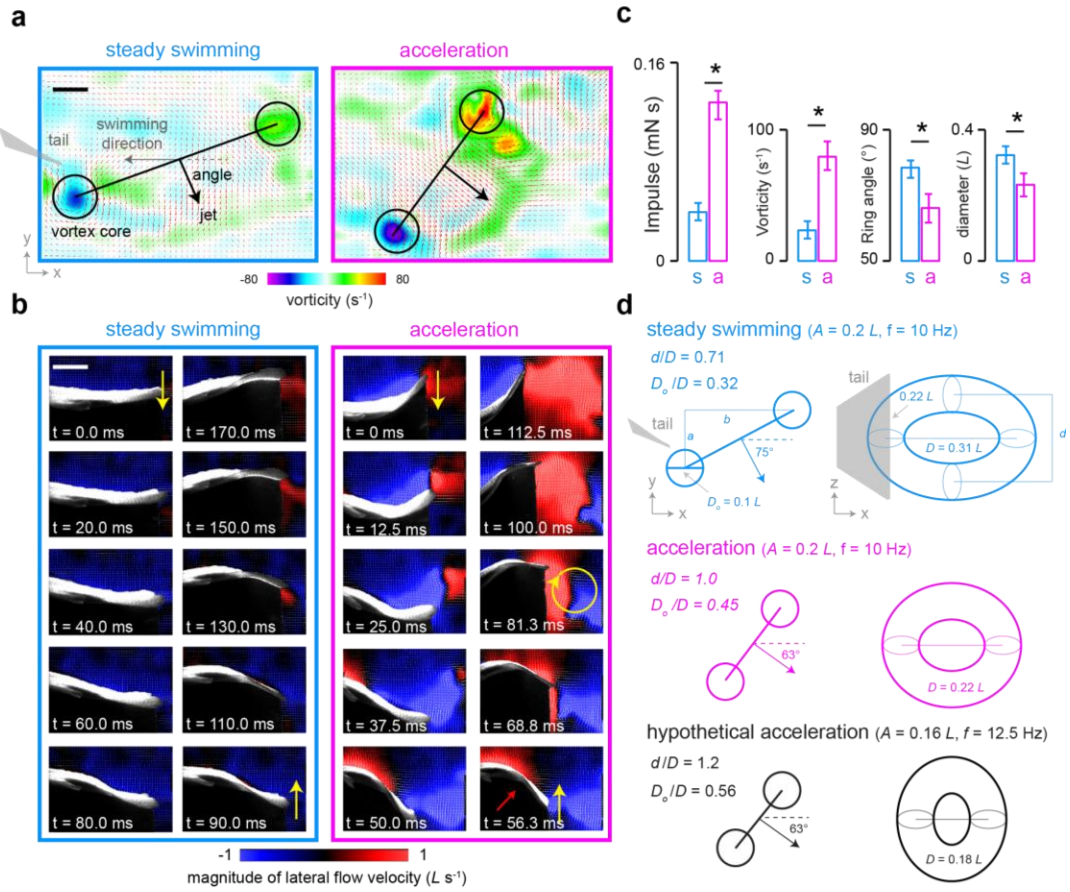


534
535

536 Figure 2.

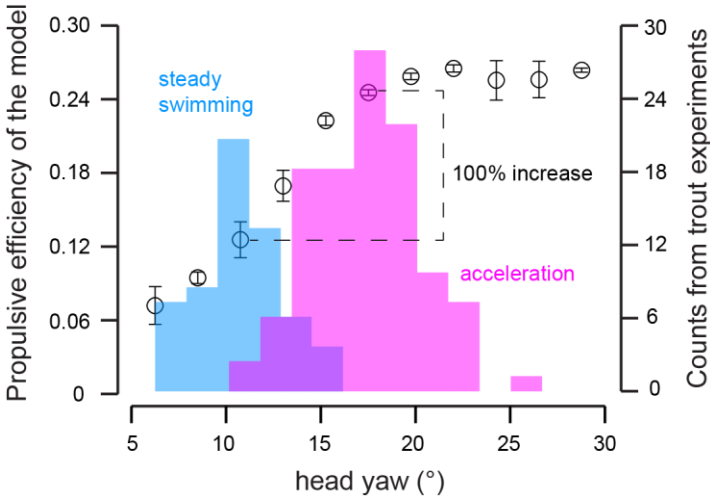
537

538



539
540

541 Figure 3.



542

Figure Legends

Figure 1. Fishes have higher tail beat amplitude during acceleration. (a) This phenomenon was confirmed across a wide range of fishes from 20 taxonomic orders with different body shapes, swimming modes and ecologies. Blue and magenta lines indicate the mean tail beat amplitudes for steady swimming ($0.181 \pm 0.004 L$) and acceleration ($0.244 \pm 0.006 L$), respectively. Mean tail beat amplitudes for steady swimming and acceleration are statistically different (unpaired T-test, $P < 0.001$). During steady swimming, it was not possible to measure the tail beat amplitude of few species (black seabass, sergeant major, pipefish, summer flounder and filefish), as they use primarily median or pectoral fins for propulsion. Error bars are \pm one standard error of the mean.

Figure 2. Hydrodynamics of steady swimming versus acceleration. (a) Representative flow fields behind a rainbow trout ($L=32$ cm) swimming steadily at $3 L s^{-1}$ (left) and accelerating (right) from the same initial speed. The heat map denotes vorticity where negative (magenta) and positive (red) values indicate clockwise and counter-clockwise rotation, respectively. The length of the scale bar is 2 cm. (b) Body movements of the same fish during steady swimming (left column) and acceleration (right column) over one representative tail beat cycle. Yellow arrows indicate the direction of tail movement. The blue and red denote the magnitude of left and right flow fields, respectively, in the fish frame of reference. In each video frame, the body of the trout is visible from the dorsal fin to the tail, which represents the 30% of the total length. The length of the scale bar is 4.5 cm. (c) Mean impulse, vorticity, angle and diameter of an average vortex ring for steady swimming and acceleration (10 tail beats from each fish, $n=2$ fish). * denotes significant at $P<0.01$, unpaired T-test. Error bars are \pm one standard error. (d) Hypothesized vortex ring geometry and orientation behind fish swimming steadily (blue) and accelerating (magenta). Hypothetical acceleration with lower tail beat amplitude is also shown for comparison (black).

Figure 3. Fishes adopt acceleration kinematics tuned for high propulsive efficiency. Propulsive efficiency of the physical model as a function of head yaw at flow speed 1.2 L s^{-1} (left axis, black points; error bars are \pm one standard error); propulsive efficiency increases with increasing head yaw. A histogram of head yaw (right axis) is shown for live trout during steady swimming (blue) and acceleration (magenta). Note that the overlapped region between the distributions steady swimming and acceleration appears darker. The average head yaw for steady swimming and acceleration is $12.469 \pm 0.370^\circ$ and $17.805 \pm 0.352^\circ$, respectively (unpaired T-test, $P < 0.01$).